Energy Conversion and Management 311 (2024) 118532

Contents lists available at ScienceDirect

Energy Conversion and Management

journal homepage: www.elsevier.com/locate/enconman

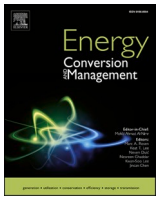

Research Paper

Hydrogen production from renewable energy resources: A case study

Gianpiero Colangelo *, Gianluigi Spirto, Marco Milanese, Arturo de Risi

University of Salento, Department of Engineering for Innovation, SP Per Monteroni, 73100 Lecce, Italy

A R T I C L E I N F O

Keywords:
Water electrolysis
Renewable energies
Hydrogen production

A B S T R A C T

In the face of increasing demand for hydrogen, a feasibility study is conducted on its production by using Renewable Energy Resources (RERs), especially from wind and solar sources, with the latter preferring photovoltaic technology. The analysis performed is based on climate data for the Province of Brindisi, Apulia, Italy. The various types of electrolyzers will be analyzed, ultimately choosing the one that best suits the case study under consideration. The technical aspect of the land consumption for RER exploitation until 2050 is analyzed for the Italian case of study and for the Apulia Region. For both the 200 MW and 100 MW RER Power Plants, an economic analysis is carried out on the opportunities for using hydrogen. In the last part of the economic analysis, the trade-off between the high specific investment cost and the Capacity Factor of Wind technologies is also investigated. The results show the affordability of building high-scale Wind Farms, harnessing the existing scale economies. The lowest Hydrogen selling price is achieved by the 200 MW Wind Farms equal to 222 €/MWh against 232 €/MWh of the 200 MW Photovoltaic (PV) Farm. Finally, the feasibility analysis considers also the greenhouse gas emission reduction by including in the economic analysis the carbon dioxide (CO_2) Average Auction Clearing Price leading for the 200 MW Wind Farms to a hydrogen selling price equal to 191.2 €/MWh against 201 €/MWh of the 200 MW Photovoltaic Farm.

Nomenclature

Abbreviations	
2 W	Two-parameter Weibull distribution function
AEMs	Alkaline anion Exchange Membranes
AWE	Alkaline Water Electrolysis
CPV	Concentrated Photovoltaic
FCEV	Fuel Cell Electric Vehicle
IRR	Internal Rate of Return
LSM	Lanthanum Strontium Manganite
NPV	Net Present Value
PEMs	Proton Exchange Membranes
PTE	Plan for the Ecological Transition
PV	Photovoltaic
RER	Renewable Energy Resources
SOE	Solid Oxide water Electrolysis
TSO	Transmission System Operator
VGV	Variable Guide Vanes
YSZ	Yttrium-Stabilized Zirconium oxide
Symbols	
G	Global Horizontal Irradiation [kWh/m^2]
G_α	Total Irradiation on Tilted Surface [kW/m^2]
G_A	Direct Horizontal Irradiation [kW/m^2]

(*continued on next column*)

(*continued*)

Abbreviations	
2 W	Two-parameter Weibull distribution function
G_d	Diffuse Horizontal Irradiation [kW/m^2]
G_o	Total Horizontal Irradiation at the top of the atmosphere [kW/m^2]
R_A	Ratio of the Direct Irradiation on Tilted Surface to Direct Horizontal Irradiation
σ	Reflection Surface Index
α	Surface Tilting Angle [deg]
θ_i	Incidence Angle of Light Rays on Titled Surface [deg]
θ_z	Zenith Angle [deg]
I_l	Light generated current [A]
N_p	Number of parallel module
I_{lr}	Light generated current of PV module at reference conditions [A]
I_o	Saturation current of PV array [A]
μ_{sc}	Temperature coefficient of PV module, [A/K]
T_{pv}	Temperature of PV module [K]
T_{pvr}	Temperature of PV module at reference conditions [K]
A_{req}	PV Array Area [m^2]
I_{mp}	Current at maximum power point [A]
V_t	Thermal voltage of PV array [V]
N_c	Number of solar cell per module
N_s	Number of PV modules in series

(*continued on next page*)

* Corresponding author.
E-mail address: gianpiero.colangelo@unisalento.it (G. Colangelo).

https://doi.org/10.1016/j.enconman.2024.118532
Received 9 October 2023; Received in revised form 6 April 2024; Accepted 7 May 2024
Available online 14 May 2024

(*continued*)

Abbreviations	
2 W	Two-parameter Weibull distribution function
K	Boltzmans constant [J/K]
q	electronic charge [C]
V_{mp}	Voltage at maximum power point [V]
V_{oc}	Open circuit voltage [V]
P_{mp}	Power at maximum power point [W]
E_{PV}	PV energy Produced [kWh]
TCF	Temperature Correction Factor
η_{PV}	Module Efficiency
η_{ele}	Electric generator Efficiency
η_{Inv}	Inverter Efficiency
$f(v)$	Probability distribution function
$F(v)$	Cumulative distribution function
k	Shape factor
c	Scale factor [m/s]
$\bar{v}$	Average wind speed [m/s]
v_{hub}	Wind Speed at Turbine Rotor Hub [m/s]
v_{10}	Wind Speed at 10 m [m/s]
h_{hub}	Rotor Hub Height [m]
ρ	rotor radius
h_{10}	10 m Height [m]
z_0	Roughness length[m]
P_{WPD}	Wind power density [W/m^2]
Γ	Gamma function
η_{Array}	Wind array efficiency
η_{Arfoil}	Wind turbine airfoil efficiency
E_{Nernst}	Nernst Voltage [V]
V_{act}	Activation Voltage [V]
V_{ohm}	Ohmic Voltage [V]
V_{con}	Mass Transportation Overpotential [V]
N_{cell}	Number of cell
V_{stack}	Stack Voltage[V]
A_{ele}	Electrode Area [m^2]
R_t	Annual Cash Flow [€]
i	Discount rate [%]
T	Project Life [years]
E_{PP}	Average Energy Produced over a year [MWh/y]
P_{rated}	Rated Power Capacity [MW]
T	Solar year

1. Introduction

Hydrogen is the most abundant element in nature and it is the basis of many industrial and technological processes. In 2021, the world demand for hydrogen was 94.3 Mt, registering an increase of 5 % compared to that recorded in 2020. Fig. 1 shows the distribution of the global demand for H_2 for the year 2021. From the graph, it is immediately clear that the petrochemical and chemical sectors alone cover 93 % of the global demand with over 87 Mt of Hydrogen used. [1].

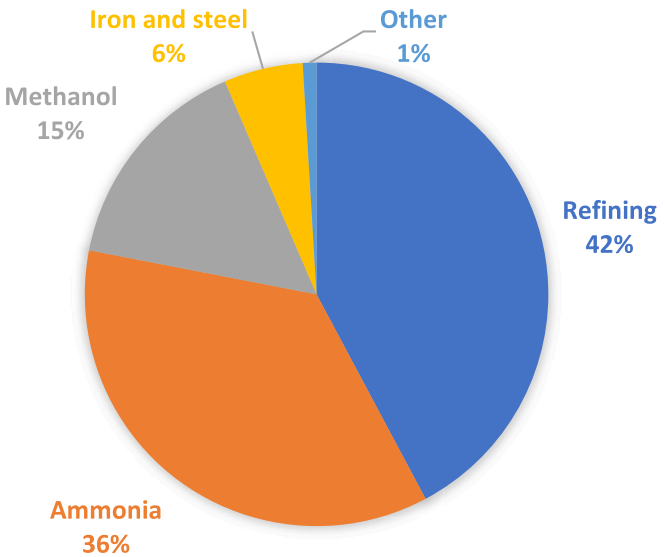

Fig. 1. Global Hydrogen repartition by sector in 2021 [1,2].

In the near future, further growth in the global demand for Hydrogen is estimated, also driven by its use in other sectors, such as in the transport and power sector as an alternative fuel, as a precursor for synthetic fuels, or as a blend with other fuels [1 2].

As regards the use of hydrogen in the transport sector, there are various projects and technologies, which try to break down the barriers that prevent the diffusion of hydrogen in this sector. According to Borgstedt et al. [3] the reasons for this delay in market penetration, compared to hybrid vehicles and electric vehicles, can be found in the complexity of the infrastructure linked to the refuelling of Fuel Cell Electric Vehicles (FCEVs), in the high complexity of this type of technology and in the significant advances made by competing technologies. Asif and Klaus Schmidt [4] who, retracing the policies in favour of FCEVs put in place by Japan, the European Union, and the United States, have highlighted how they are nonetheless giving a stimulus to the development of this technology and they are reducing costs, although these policies are overlapping in certain regions.

An increase in the demand for hydrogen is expected in the power sector, due not only to a growing demand for global energy but also to the need for an energy transition that envisages the gradual replacement of fossil fuels as the primary source of energy. Chiesa et al. [5] have investigated the possibility of using hydrogen as a fuel in gas turbines. The authors concluded that a gas turbine substantially requires few precautions to be reused with the new fuel; in particular, a dilution of the hydrogen is required, through N_2 or steam, to limit the flame temperature, and therefore the production of NO_X. Similarly, Xiao et al. [6] studied the use of a blend of ammonia and hydrogen as an alternative fuel in a gas turbine. In particular, the authors studied the chemical-kinetic behaviour of an ammonia/hydrogen mixture in premixed combustion, verifying the production of NOx through the Mathieu mechanism at different compositions and pressures.

Therefore, it is evident that with an ever-increasing demand for Hydrogen, it is necessary to produce it from an alternative source to the current and predominant one linked to fossil fuels. For example, the use of Renewable Energy Resources (RER) which, via water-electrolysis, can produce hydrogen to be used directly as a fuel in gas-fired plants, stationary fuel cells, FCEVs, or as a methane or ammonia blend.

Incer-Valverde et al. [7] review the literature analysing the state of the art of process using “green” hydrogen as an energy carrier. They evaluate the different options applied to the Germany case study finding as promising solutions the Power-to-Ammonia, Power-to-Methanol, Power-to-Hydrogen and Power-to-Liquid hydrogen processes. In these four processes, the authors considered hydrogen produced by electrolysis fed RER.

Hafsi et al. [8] perform a comparative study on an isolated direct current micro-grid, which consists of two primary sources, a photovoltaic and wind turbine generator, an energy storage system and a backup device based on Proton Exchange Membrane Fuel Cell. The study conducted by Oldenbroek et al. [9] aims to verify the feasibility of a city completely powered by solar and wind power, with hydrogen and electricity as energy carriers. The energy in excess, which does not cover the power and heat needs, is used via water-electrolysis to produce hydrogen to be used directly in the supply network of the fuelling stations for the FCEVs or stored in underground storage. On the contrary, when the energy demand cannot be satisfied by renewable sources, then the Hydrogen contained in the tanks of the FCEVs can be used to make up for the energy deficit. The results demonstrate that the energy model is reliable and that the off-peaks of demand never exceed 50 % of the FCEVs fleet.

Temiz et al. [10] study the possibility of developing a hydrogen energy system based on solar and wind resources for remote communities. They assess a feasibility analysis evaluating three different renewable electricity generation options namely, wind farm, bifacial photovoltaic plant and floating photovoltaic plant coupled with an

anion exchange membrane (AEM) electrolyser, for hydrogen generation, and a proton exchange membrane (PEM) fuel cell, in order to use the hydrogen, in a case study for Cochrane, Ontario, Canada. The results show as for a community with 5300 people the integrated system can achieve overall energy and exergy efficiencies respectively of 37.68 % and 36.69 % in a typically selected meteorological year.

The present paper aims to investigate whether with the technologies currently available for the exploitation of the RERs it is possible to create an alternative model to the production of hydrogen from fossil fuels and analyse the environmental sustainability of this choice. According to the Gestore dei Servizi Energetici (GSE) 2021 Report of Electricity produced from RER in the Apulia Region, 49.7 % of the electricity produced from RER is from the wind resource, followed by the solar resource with 36.6 % of the electricity produced from RER [11]. The data of the other RER exploited in the Apulia Region are shown in Table 1. These data reflect the abundance of wind and solar resources in Apulia Region and among the RERs wind and solar are the technical solutions with the highest installed capacity and lowest levelized cost of electricity [10], indeed through the RETScreen Analysis Software [12] is carried out a technical–economic feasibility analysis in a case study for the Province of Brindisi, Apulia Region, Italy.

The impact on land consumption is among the most relevant environmental aspects in the exploitation of the RERs and a study on land transformation has been carried out starting from the year 2000 to 2050 through the software LEAP [13]. The analysis of the technical–economic feasibility of wind and solar-powered systems dedicated to the production of hydrogen, jointly with the analysis of the evolution of land consumption linked to the wind and solar resources exploitation, both on a national and regional basis, is the main difference if compared to the openly available literature studies. In fact, there is a lack of empirical knowledge of how renewable resource exploitation is related to land consumption. Therefore, the present paper aims to close this gap in the literature by realizing a wind and solar powered plant for hydrogen production, capturing the land consumption effect of exploiting these two renewable resources which are the most abundant in this part of Italy.

2. Solar resource analysis

The Province of Brindisi presents a good susceptibility to the exploitation of solar sources, in fact, the National Agency for New Technologies, Energy and Sustainable Economic Development (ENEA) by collecting data on global solar radiation on the ground on a horizontal plane, G, of 243 Italian localities in the period from 2006 to 2020. ENEA calculates an average annual G of 1597.3 kWh/m^2 for Brindisi, classifying it as the 43rd location with the highest Italian G. Fig. 2 shows the trend of the daily monthly averaged G for the Province of Brindisi [14].

From the G is possible to calculate the total irradiance on tilted plane G_α using the Hay's sky diffusion anisotropic model (Eq. (1)) [15]:

$$G_\alpha = G_A R_A + 0.5\sigma G(1-\cos\alpha) + G_d\left[R_A\frac{G_A}{G_o} + 0.5\left(1-\frac{G_A}{G_o}\right)(1+\cos\alpha)\right] \quad (1)$$

where

Table 1
Electricity produced from RER in Apulia Region in 2021.

RER	Energy produced (ktep)
Wind	453
Solar PV	334
Bioenergy	124
Hydropower	1
Geothermal	0

$$R_A = \frac{\cos\theta_i}{\cos\theta_z} \quad (2)$$

From (Eq. (1)) it is possible to calculate the light-generated current, I_l, and the current at the maximum power point, I_{mp}, of a PV array [16]:

$$I_l = N_p\left(\frac{G_\alpha}{G}\right)\{I_{lr} + \mu_{sc}(T_{pv} - T_{pvr})\} \quad (3)$$

$$I_{mp} = I_l\left(1-\left(1-\frac{V_t}{V_{mp}}\right)\right) \quad (4)$$

where:

$$V_t = \frac{N_c \bullet N_s \bullet K \bullet T_{pv}}{q} \quad (5)$$

$$V_{mp} = V_{oc} - V_t\ln\left\{1+\left(\frac{V_{mp}}{V_t}\right)\right\} \quad (6)$$

$$V_{oc} = V_t\ln\left\{1+\left(\frac{I_l}{I_o}\right)\right\} \quad (7)$$

Combining (Eq. (4)) and (Eq. (6)) it's possible to obtain the power at maximum power point, P_{mp}, [16]:

$$P_{mp} = V_{mp}I_{mp} \quad (8)$$

Finally, it's possible to obtain the size of the PV array using (Eq. (9)) [17]:

$$A_{req} = \frac{E_{PV}}{G_\alpha \bullet TCF \bullet \eta_{PV}\eta_{Inv}} \quad (9)$$

3. Wind resource analysis

Milanese et al. [18] starting from the California Meteorological Model (CALMET [19]) developed a numerical method called WEST (Wind Energy Study of Territory) which reconstructs the wind fields. The result of the study is a map of the wind power density of the region Apulia which can help to identify the preliminary site of interest for the realization of a wind farm. According to the results of the study, the chosen site for the wind farm realization is characterized by a value of wind power density of about 394 W/m^2 measured at 100 m height. Furthermore, these wind data classified the site in the Province of Brindisi as suitable for a wind turbine class II as per IEC 61400–1 [20]. This classification is defined in terms of the annual average wind and class II represents a medium wind speed, confirming the site is eligible for a good exploitation of wind resource.

To precisely determine the quality of the site wind source, an annual measurement campaign was carried out and it is represented in Fig. 3.

From these measurements, obtained at a height of 10 m, it is possible to derive the two-parameter Weibull distribution (2 W) used to describe the distribution of wind speeds $f(v)$ (Eq. (10)) at a given site:

$$f(v) = \left(\frac{k}{c}\right)\left(\frac{v}{c}\right)^{k-1}e^{-\left(\frac{v}{c}\right)^k} \quad (10)$$

From the distribution $f(v)$ it is possible to obtain the cumulative distribution function $F(v)$ (Eq. (11))

$$F(v) = \int f(v)dv = \left(\frac{k}{c}\right)\left(\frac{v}{c}\right)^{k-1}e^{-\left(\frac{v}{c}\right)^k} = \int\left(\frac{k}{c}\right)\left(\frac{v}{c}\right)^{k-1}e^{-\left(\frac{v}{c}\right)^k} = 1-e^{-\left(\frac{v}{c}\right)^k} \quad (11)$$

Starting from the sample represented by the measurement campaign conducted on the site of interest, it is possible to estimate the parameters k and c characteristic of the 2 W distribution through (Eq. (12)) and (Eq.

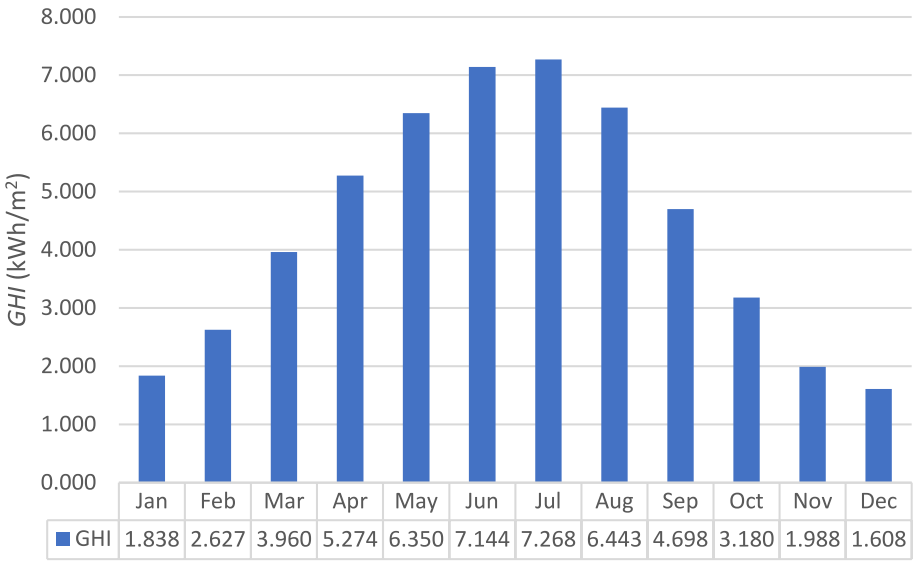

Fig. 2. Annual Site Daily Monthly Averaged *G*.

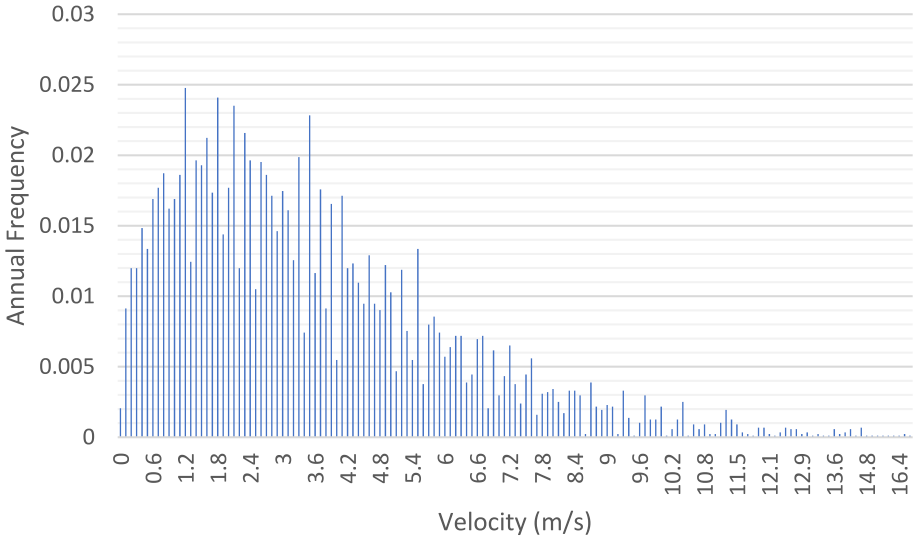

Fig. 3. Annual site wind speed measurement campaign taken at 10 m height.

(13)):

$$k = \left(\frac{\sum_1^n v_i^k \ln(v_i)}{\sum_1^n v_i^k} - \frac{\sum_1^n \ln(v_i)}{n} \right)^{-1} \tag{12}$$

$$c = \left(\frac{1}{n} \sum_1^n v_i^k \right)^{-1/k} \tag{13}$$

Thus, a value of $k = 1.4018$ and $c = 3.872$ is obtained.

Having found the characteristic parameters of the distribution $f(v)$, it is now possible to calculate the probable wind speed expected at the site of interest through (Eq. (14)):

$$\bar{v} = c\left(1 + \frac{1}{k}\right)^{1/k} \tag{14}$$

Thus a value of $\bar{v} = 5.68 m/s$ is obtained. [21–24].

Furthermore, since the wind speed measurement campaign was carried out at a height of 10 m, it is necessary to take into account the viscous stresses due to the roughness of the ground, therefore using (Eq. (15)) it is possible to calculate the effective wind speed at the rotor hub of the turbine [25,26]:

$$v_{hub} = v_{10}\left(\frac{\ln(h_{hub}/z_0)}{\ln(h_{10}/z_0)}\right) \tag{15}$$

To calculate the electrical power produced by the wind farm it is necessary to calculate first the wind power density, P_{WPD}, [21,24]:

$$P_{WPD} = \left(\frac{P}{A}\right)_W = \int_0^\infty \frac{1}{2}\rho v^3 f(v) dv = \frac{1}{2}\rho c^3 \Gamma\left(1 + \frac{3}{k}\right) \tag{16}$$

Finally, the electric power is obtained by the equation accounting for the efficiencies of the plant:

$$P_{el} = P_{WPD} \bullet \eta_{Arfoil} \bullet \eta_{ele} \bullet \eta_{Inv} \tag{17}$$

4. Project technical feasibility

The system proposed in Fig. 4 for the exploitation of renewable resources, which would be placed at the Brindisi site, consists of a 50 MW PV plant, a 50 MW wind farm, an electrolyzer, responsible for the production of hydrogen, and a compressor. The hydrogen thus produced

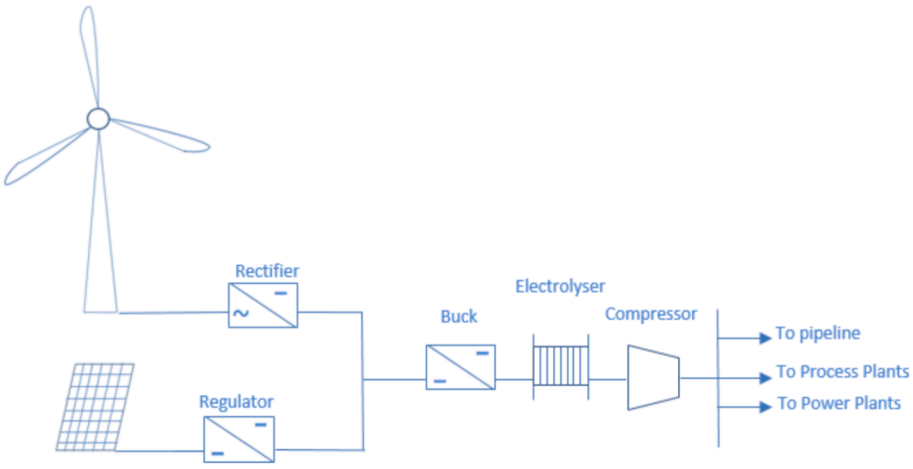

Fig. 4. Schematic Hydrogen Production Plant.

can then be sent directly to hydrogen pipelines or, equivalently, as a blend, for example with methane. Despite hydrogen embrittlement being a phenomenon well known due to the hydrogen presence in steel [27,28], the use of hydrogen blend over the 10 % or pure hydrogen is possible by limiting pressure and moisture, respectively, to 21 MPa and to 20 ppm in the temperature range from − 62 °C to 232 °C as per ASME B31.12 standard [29]. The feasibility of hydrogen blend with methane was tested by Snam, the Italian Transmission System Operator (TSO). Snam injected a hydrogen blend of up to 10 % into the network in Contursi demonstrating the possibility to transport hydrogen over more than 20,000 km of pipeline [28,30].

In Cerniauskas et al. [31] a technical–economic analysis is performed on the possibility of reconverting the existing gas pipeline network in Germany to hydrogen transport. The results show that more than 80 % of the German national network can be used for the transport of hydrogen and this solution can lead to transport cost savings of between 20 %-60 %, compared to the case of a new construction of an infrastructure used for the transport of hydrogen.

Another solution for its use is to exploit it in Gas Power plants or as a reagent in the Petrochemical or Chemical Process.

Furthermore, to evaluate the influence of possible scale economies, the case of a 100 MW PV solar plant and 100 MW wind farm has been studied.

4.1. Photovoltaic solar system

Liang Jiang et al. [32] performed a comparison between the monocrystalline silicon technology and the polycrystalline silicon technology as these two technologies dominate the PV system market. They demonstrated how the slightly higher monocrystalline investment cost is compensated by the higher power performance due to the module's weak internal resistance and the high conversion of the incident photons to electrons.

To realize the PV system, monocrystalline silicon technology was considered, more mature and with higher efficiency than the other PV technologies. To better adhere to the reality a commercial mature product is preferred and to evaluate the real applicability of the project, only the companies with the major shares of PV module market have been taken into account. Analyzing the top 15 worldwide PV module manufacturers [33] on the RETScreen database [12], the SunPower SPR-X2-345 has been taken into account for its high specific power production and high efficiency. Table 2 shows the technical specifications of the PV modules used for both 50 MW and 100 MW PV solar plants.

Table 2
PV module technical data.

PV Module Technical Data	
Manufacturer	SunPower
Model	SPR-X21-345
Nominal Power (W)	345
Module area (m^2)	1.538
Open-circuit voltage (V)	68.2
Short-circuit current (A)	6.39
Rated voltage (V)	57.3
Rated current (A)	6.02
Average efficiency (%)	21.5
Power temperature coefficient (%/°C)	−0.29
Voltage temperature coefficient (mV/°C)	−167.4
Current temperature coefficient (mA/°C)	2.9

4.2. Wind farm specification

Considering the measurement campaign and the data analysis carried out, the site can be classified as IEC Class II according to IEC 61400. Therefore, following the same design principle used for the PV Solar System, only the wind turbine market key companies have been taken into account [34]. Among them in RETScreen database [12], the one that better matches the wind characteristics of the site is the Wind Turbine in Table 3, Vestas V90-1.8 was chosen to build the 50 MW and 100 MW Wind Farm.

Table 3
Wind Turbine Technical Data.

Wind Turbine Technical Data	
Power capacity per turbine (kW)	1,800
Manufacturer	Vestas
Model	V90-1.8
Wind Class	IEC II
Hub height (m)	105
Rotor diameter per turbine (m)	90
Swept area per turbine (m^2)	6.362
Cut-in wind speed (m/s)	4
Rated wind speed (m/s)	12
Cut-out wind speed (m/s)	25
Number of blades	3
Shape factor	1.4
Array losses (%)	4
Airfoil losses (%)	2
Miscellaneous losses (%)	6

4.3. Electrolyzer

The water electrolysis process is one of the alternative methods for the production of hydrogen without the aid of fossil fuel. Other hydrogen production methods, for example, are the harnessing of radiations. Imran et al. [35] investigate the application of radiations in water splitting, analysing future perspectives and safety measures. However, electrolysis is the most mature technology in hydrogen production by water. This process is based on the reverse reaction of the formation of H_2O starting from H_2 and O_2 (Eq. (18)). This reaction is strongly exothermic, as shown by the values of ΔH_f^0 and ΔG_f^0, therefore it derives a high energy requirement to be able to carry out the reverse reaction.

$$2H_2(g) + O_2(g) \leftrightarrow 2H_2O(g) \Delta H_f^0 = -241.8 \frac{kJ}{mol}; \Delta G_f^0 = -228.6 \frac{kJ}{mol} \tag{18}$$

The water electrolysis process is carried out by means of an electrolyzer and it is composed of three fundamental elements: a cathode, an anode, and an electrolyte. The H_2 formation reaction takes place on the cathode (Eq. (19)), while O_2 is released on the anode (Eq. (20)), the set of reactions (Eq. (19)) and (Eq. (20)) allows the reverse reaction represented in (Eq. (18)) to take place.

$$4H^+(g) + 4e^- \rightarrow 2H_2 \tag{19}$$

$$2H_2O(l) \rightarrow O_2(g) + 4H^+(g) + 4e^- \tag{20}$$

The passage of electrons occurs through the circuit connected to the two electrodes of the electrolyzer, while the passage of ions occurs through the electrolyte. Based on the different characterization of the electrolyte and the transported ions, it is possible to distinguish the different types of electrolyzers, such as alkaline water electrolysis (AWE), proton exchange membranes (PEMs) and solid oxide water electrolysis (SOE). Among the AWEs it is possible to distinguish subcategorization known as alkaline anion exchange membranes (AEMs), they have the same charge carrier as the AWEs, but a solid (polymeric) electrolyte like the PEMs.

AWEs consist of a family of electrolyzers consisting of an electrolyte composed of a solution of distilled water and 20 %-40 % sodium hydroxide or potassium hydroxide surrounding an asbestos diaphragm. The AWEs operate at low temperatures (40–90 °C) and have the advantage of generating H_2 with a degree of purity equal to 99 % with a power consumption of 4.5–5.5 kWh/Nm^3 and an efficiency of about 60 %.

On the other hand, in PEMs the liquid electrolyte is replaced by a solid one, consisting of a sulfonated polystyrene membrane. The solid membrane has the advantage of having a lower gas permeability than the AWEs asbestos diaphragm, furthermore by eliminating the KOH or NaOH-based solution, the alkaline fog, which forms during the electrolysis process, is also missing. PEMs also have the advantage of responding faster to transients than AWEs [36,37].

Regarding the SOE, Wolf et al. [38] reviewed the state-of-the-art of this technology. In particular, the SOE is capable of achieving high efficiencies of up to 100 % due to the high operating temperatures which allow advantageous thermodynamics and reaction kinetics. Indeed the yttrium-stabilized zirconium (YSZ) oxide and lanthanum strontium manganite (LSM) based electrodes can operate at 700–900 °C with > 0.5–1.0 A cm^{-2}. Moreover, high-temperature electrolysis triggers also degradation mechanisms which lead to microstructural change and consequent loss of performance and the major challenge of the research in SOE is the long-term stability of electrodes, which is also the major barrier to its commercialization. Despite the research effort to develop different combinations of alternative electrode materials to avoid degradation mechanism at high operating temperatures, Wolf et al. [38] underline the lack of long-term (>5000 h) durability tests, necessary to prove the technology's readiness for future commercialization.

Table 4 shows the different types of electrolyzers with the relative operating temperatures, the construction characteristics of the electrodes, and the respective reactions.

The behavior of an electrolyzer is described by the Voltage-Current density curve. The voltage across a cell is described by the relationship expressed in (Eq. (21))

$$V_{cell} = E_{Nernst} + V_{act} + V_{ohm} + V_{con} \tag{21}$$

From (Eq. (21)) it follows that the voltage required across the two electrodes to be able to start the electrolysis process increased with respect to the voltage required by the ideal process. In fact, because of the presence of different overvoltages linked to different physics mechanisms, the voltage is higher than Nernst's potential. It can be distinguished between three different overvoltages. The activation overvoltage is necessary for the electrodes to be able to initiate the transfer of electrons and ions. The overvoltage derives from the electrical resistance due to the passage of charges. Finally, the overvoltage is due to the mass transfer inherent in the products of the electrolysis process.

Consequently, the voltage of the stack can be expressed by (Eq. (22)), if the stack consists of N serial cells; otherwise, (Eq. (23)) applies in case of parallel configuration:

$$V_{stack} = N_{cell} \bullet V_{cell} \tag{22}$$

$$V_{stack} = V_{cell} \tag{23}$$

In order to be able to extrapolate the behaviour of the cell voltage as a function of the current density, various empirical and semi-empirical models have been developed, such as the semi-empirical model of Ulleberg modified with the dependence of the temperature (Eq. (24)):

$$V_{cell} = E_{Nernst} + \left(\frac{r_1 + r_2 \bullet T}{A_{ele}}\right) \bullet I_{cell} + s \bullet \log\left[\left(\frac{k_1 \bullet T^2 + k_2 \bullet T + k_3}{A_{ele} \bullet T^2}\right) \bullet I_{cell} + 1\right] \tag{24}$$

The parameters r, k and A_{ele} depend on the temperature, while the parameter s is taken as a constant [39].

Finally, it is possible to express through (Eq. (25)) the efficiency of the electrolytic cell as a function of the energy expended for the production of hydrogen [40]:

$$\eta_{ele} = \frac{HHV_{H_2}}{C_E} \bullet 100 \tag{25}$$

$$C_E = \frac{\int_0^{\Delta t} N_{cell} V_{cell} I_{cell} dt}{\int_0^{\Delta t} f_{H_2}} \tag{26}$$

Combining the characteristics of each type of electrolyzer with a non-stationary power supply, such as that deriving from RER, can be difficult and limit the performance deriving from its use.

El-Shafie [41] investigates the state of the art of the different technologies used for electrolysis. The conclusions of the analysis show that AWE are the most mature and widely used technology in process applications, however, the uncertainty of the renewable source and the related power fluctuations have negative repercussions on the efficiency of the electrolyser. PEM technology, while retaining better performance in power transient conditions compared to AWE, still has higher costs which are the main barrier to broad market penetration. AEM technology, on the other hand, uses less expensive materials than PEM and has a lower cost, however, its performance is still low and requires further improvements before being used for large-scale hydrogen production.

Mohammadi and Mehrpooya [42] have analyzed the possible

Table 4
Electrolyzers characteristics [36–38,43,44].

Operation principles	Low Temperature Electrolysis			High Temperature Electrolysis		
	Alkaline (OH^-) electrolysis		Proton Exchange (H^+) electrolysis	Oxygen ion (O^{2-}) electrolysis		
	Liquid	Polymer Electrolyte Membrane		Solid Oxide Electrolysis (SOE)		
	Conventional	Solid alkaline	H^+ PEM	H^+ SOE	O^{2-} SOE	Co-electrolysis
Charge carrier	OH^-	OH^-	H^+	H^+	O^{2-}	O^2
Temperature	20 – 80 °C	20–200 °C	20–200 °C	500–1000 °C	500–1000 °C	750–900 °C
Pressure	< 30 bar		< 200 bar	< 20 bar	< 20 bar	< 20 bar
Electrolyte	Liquid	Solid (polymeric)	Solid (polymeric)	Solid (ceramic)	Solid (ceramic)	Solid (ceramic)
Anodic reaction	$4OH^-\rangle 2H_2O + O_2 + 4e^-$	$4OH^-\rangle 2H_2O + O_2 + 4e$	$2H_2O^-\rangle 4H^+ + O_2 + 4e^-$	$2H_2O^-\rangle 4H^+ + O_2 + 4e^-$	$O^{2-}\rangle 1/2O_2 + 2e^-$	$O^{2-}\rangle 1/2O_2 + 2e^-$
Anodes	Ni > Co > Fe (oxides) Perovskites: $Ba_{0.5}Sr_{0.5}Co_{0.8}Fe_{0.2}O_{3-\delta}$, $LaCoO_3$	Ni-based	IrO_2, RuO_2, $Ir_xRu_{1-x}O_2$Supports:TiO2, ITO, TiC	Perovskites with protonic-electronic conductivity	$La_xSr_{1-x}MnO_3$ + Y-Stabilized ZrO_2 (LSM-YSZ)	$La_xSr_{1-x}MnO_3$ + Y-Stabilized ZrO_2 (LSM-YSZ)
Cathodic reaction	$2H_2O + 4e^-\rangle 4OH^- + 2H_2$	$2H_2O + 4e^-\rangle 4OH^- + 2H_2$	$4H^{+-} + 4e^-\rangle 2H_2^-$	$4H^{+-} + 4e^-\rangle 2H_2^-$	$H_2O + 2e^-\rangle O^{2-} + H_2$	$H_2O + 2e^-\rangle O^{2-} + H_2$ $CO_2 + 2e^-\rangle CO + O^{2-}$
Cathodes	Ni alloys	Ni, Ni-Fe, $NiFe_2O_4$	Pt/C MoS_2	Ni-Cermets	Ni-YSZ Subst. $LaCrO_3$	Ni-YSZ perovskites
Efficiency	59–70 %	–	65–82 %	up to 100 %	up to 100 %	–
Voltage	1.8–2.4 V	≤ 0.65 V	1.8–2.2 V	0.7–1.5 V		
Current density	0.2–0.4 A/cm^2		0.6–2 A/cm^2	0.3–2 A/cm^2		
Applicability	Commercial	Laboratory	Near-term commercialization	Laboratory scale	Demonstration	Laboratory scale
Capital Cost	880–1650 USD/kW	–	1540–2550 USD/kW	> 2000 USD/kW		–
O&M Cost (% of investment/ year)	2–3	–	3–5			–
Advantages	Low Capital Cost, stable operation, mature technology	Combination of alkaline and H^+-PEM electrolysis	Compact design, fast response/start-up, high-purity H_2	Enhanced kinetics, thermodynamics: lower energy demands, high efficiency low capital cost		+direct production of syngas
Disadvantages	Corrosive electrolyte, gas permeation, slow dynamics	Low OH^- conductivity in polymeric membranes	High cost polymeric membranes; Noble metals	Mechanical instability of electrodes due to cracking, safety issues		

configurations of electrolyzers coupled with different RERs and have demonstrated how, for the solar source and the wind source, it is more advantageous to combine them with an alkaline electrolyzer.

5. Land consumption

Another phenomenon to take into consideration in the exploitation of hydrogen from renewable sources is the impact of these technologies on land consumption. In Italy, the Gestore dei Servizi Energetici (GSE) has estimated an average specific land occupation for PV Systems of 18.6 m^2/kW, therefore a 50 MW PV Solar Plant would require 93 ha for its construction [45].

As far as wind power technology is concerned, the construction of new plants must comply with various national and regional regulations, therefore the land consumption is highly uneven, as shown in Table 5. Furthermore, the construction of a wind farm requires considerable distance between one turbine and another, so as not to interfere with the fluid dynamics of the air masses used. According to Milanese et al. [46], the fluid dynamic perturbation due to the mutual position of wind turbines ends generally within 500 m of the wind turbine discharge.

To evaluate the technical land consumption for the exploitation of the wind source there are various empirical rules, which are more easily to apply for a preliminary feasibility analysis. Kipp equation (Eq. (27)), ensures a conservative approach in the calculation of land consumption, calculating the minimum area required by a wind turbine [47].

$$A_{req} = \pi(h_{hub} + \rho)^2 \tag{27}$$

Applying (Eq. (27)), for a 50 MW wind farm approximately 353 ha are required, it is, therefore, clear how the intensive exploitation of the RER involves considerable use of land.

Table 5
Wind Farm Power Distribution in Italian Regions [34].

Italian Region	Wind Farms Power shares
Piedmont	0.2 %
Aosta Valley	0.1 %
Lombardy	0.1 %
Trentino-Alto Adige	0.1 %
Veneto	0.1 %
Friuli-Venezia Giulia	0.1 %
Liguria	0.6 %
Emilia-Romagna	0.3 %
Tuscany	1.3 %
Umbria	0.1 %
Marche	0.2 %
Lazio	0.6 %
Abruzzo	2.5 %
Molise	4 %
Campania	14.4 %
Apulia	25.8 %
Basilicata	9.2 %
Calabria	10.9 %
Sicily	19.1 %
Sardinia	10.7 %

In addition to affecting land consumption, the construction of new plants for the harnessing of RER triggers other mechanisms that indirectly affect soil consumption, such as the phenomenon of territorial fragmentation. Fragmentation generates portions of territory blocked by road and traffic infrastructure serving new plants or settlements and causes serious repercussions in terms of land consumption and

ecosystem services [48,49].

From the 4th Report on Circular Economy in Italy [50] it emerges how in Italy between 2010 and 2019 the consumption of renewable energy grew so much as to be the second European country for the consumption of renewable energy after Spain. On the other hand, Italy presents one of the worst performances among the 27 European Union states in terms of Land Consumption presenting 7.1 % of its surface covered by artificial structures against 3.6 % in Poland, 3.7 % in Spain and 5.6 % in France.

However, it appears evident that in order to achieve the objectives linked to the energy transition, strong exploitation of the RER is required. The Plan for the Ecological Transition (PTE), put in place by Italy, foresees that by 2030 72 % of the energy produced will come from renewable sources, a share destined to rise to 95–100 % in 2050. To achieve these objectives the PTE relies mainly on the exploitation of photovoltaic technology. In terms of land consumption, it will therefore be essential to resort to the exploitation of surfaces from buildings, a solution already contemplated by the PTE to protect the territory[51].

To better understand the dynamics of land transformation in Italy, it is essential to understand the subdivision and classification of soil surfaces and their evolution over the years on a national basis, historically characterizing the flows from one class to another.

In this sense, the Higher Institute for Environmental Protection and Research (ISPRA) analysed the Italian territorial composition and its evolution from the 1960 s to 2017, identifying in Table 6 the flows between the different soil classes that have characteristics and characterize the Italian territory [52].

Table 7 shows the territorial composition at regional level for the various land classes, the data refer to 2017.

By combining the data relating to land coverage and the transformations of the soils that have occurred, with data relating to the exploitation of the RER since the 2000 s, it is possible to establish the share of land consumption relating to the use and construction of RER power plants. In Fig. 5 it is possible to find respectively the Italian annual electricity production from solar sources and that from wind sources. Based on this information, it is possible to estimate the impact of the RER harnessing on the transformations in the Italian territory in the coming years and consequently to calculate the possible future trend of land coverage up to 2050. The analysis is performed with the help of the software LEAP [13].

5.1. Results

The hypotheses underlying the analysis are based on the current policies adopted by Italy in support of RER, in particular, this study wants to focus mainly on ground-mounted solar photovoltaic and onshore wind turbines, and on the current technological level reached by the technologies under consideration. It is reasonable to consider that as regards wind energy technology, as well as for monocrystalline and polycrystalline technology of solar photovoltaics, technological development has reached the level of maturity, therefore it will be difficult to find improvements or, in any case, if they occur, they will not be such as to upset the analysis carried out.

A separate discussion, however, is to be made on the policies in the field of energy transition which can be adopted in general by the various countries. They can heavily affect the analysis carried out both as regards the cost analysis and as regards the transformations and consumption of land. The analysis aims to investigate the sustainability and the consequences on land consumption if only these two traditional and commercial solutions are exploited.

Fig. 6 **(a)** shows the annual surface transformations affecting the

Table 6
Estimation of the percentage distribution among the main land cover changes [52].

	From Rural to Urban	From Rural to Natural	From Natural to Urban	From Natural to Rural
1960–1990	13.3 %	39.3 %	2.8 %	44.6 %
1990–2000	50.4 %	43.4 %	2.5 %	3.7 %
2000–2006	83.9 %	4 %	5.3 %	6.9 %
2006–2012	62.3 %	12 %	4.4 %	21.4 %
2012–2017	56.3 %	15.6 %	4 %	24.1 %

Table 7
Regional distribution of the Land Coverage [52].

Region	Urban Land Coverage (ha)	Rural Land Coverage (ha)	Natural Land Coverage (ha)
Piedmont	135,836	1,083,960	1,320,267
Aosta Valley	4,666	25,044	296,493
Lombardy	277,424	1,112,721	997,707
Trentino-Alto Adige	29,336	170,247	1,160,912
Veneto	169,595	1,018,659	645,402
Friuli-Venezia Giulia	62,345	297,733	431,056
Liguria	27,527	90,987	423,466
Emilia-Romagna	125,117	1,496,034	624,139
Tuscany	111,910	1,021,348	1,165,487
Umbria	30,079	426,251	389,087
Marche	44,804	596,693	296,771
Lazio	111,603	964,540	644,117
Abruzzo	32,784	479,554	567,402
Molise	8,172	272,284	163,560
Campania	102,493	744,026	513,392
Apulia	105,958	1,554,817	274,665
Basilicata	15,876	567,356	415,922
Calabria	56,408	722,036	729,834
Sicily	130,480	1,757,860	683,591
Sardinia	72,088	1,107,623	1,232,120
Italy	1,654,502	15,509,775	12,975,448

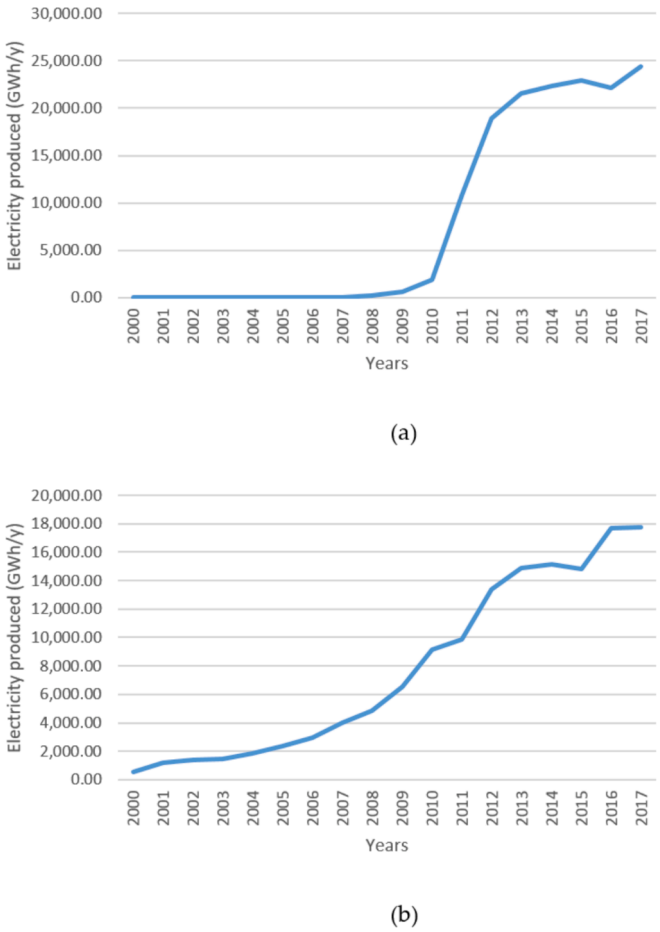

Fig. 5. Annual electricity from RER generation in Italy: (a) Solar (b) Wind [53].

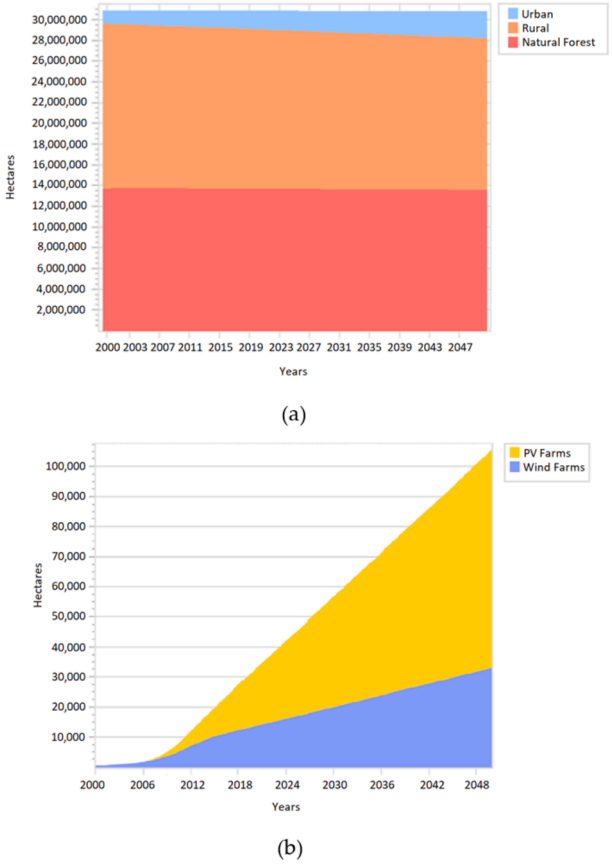

Fig. 6. Land distribution in Italy: (a) Annual land conversion (b) Annual land conversion of PV and Wind farms.

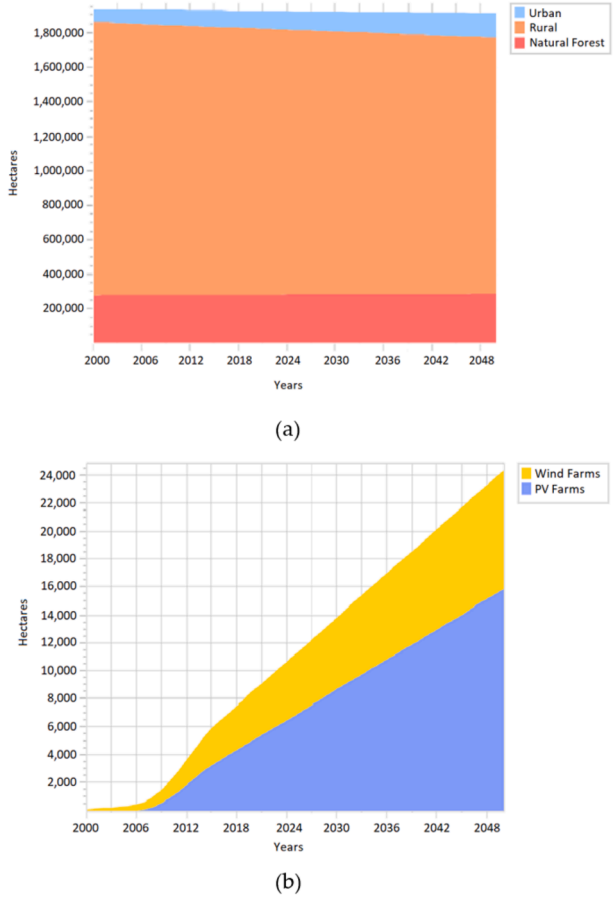

Fig. 7. Land distribution in Apulia: (a) Annual land conversion (b) Annual land conversion of PV and Wind farms.

Rural, Urban and Agricultural land classes from the years 2000 up to 2050.

Fig. 6 **(a)** shows how the urbanization process started in the 2000 s continues for the entire period considered by the analysis, in the same way, it is evident how the internal transformations between the various land classes are zero-sum as regards the Natural Forests. The land class that feeds the urbanization process is that which involves rural land, for which a continuous decrease in the available surface area is observed, so much so that from 2018 to 2050, the analysis performed estimates a loss of more than 1.2 million hectares of rural land.

On the other hand, Fig. 6 **(b)** shows how part of the conversion of the rural land mentioned above is, instead, destined for an ever-increasing share of land destined to host photovoltaic and wind power plants.

In particular, it can be seen how the growth of the portions of land intended for photovoltaic plants is greater than the portion intended for wind farms, this is also due to the problems related to the more complex authorization regime, made up of national and regional regulations, which must undergo the construction of a new wind farm.

From the data used for the national analysis, it is possible to extrapolate, through the same model created with the LEAP software, the trend of the territorial transformations of the Apulia region up to 2050. The model confirms the trend of the transformations that take place at National, as can be seen from the graphs in Fig. 7. Also for the Apulia region, the soil class most used for the construction of RER plants is the Rural one, in particular, the model estimates that in the period 2018–2050 there will be a loss of about 60,000 ha of agricultural land. The predictions of the model found a first partial confirmation of what was estimated by the survey conducted by ISPRA [51]. In the period 2006–2021, ISPRA detected a loss of approximately 5,400 ha of agricultural land in favor of the construction of ground-based PV Power Plants, in line with what was calculated with the model and with what is represented in Fig. 7. The proposed model makes it possible to calculate the use of land in the reference period 2018–2050 also with regard to wind farms, estimating it at around 8.9 % of the 60,000 ha deriving from the agricultural land class, against 19 % represented by PV farms. In fact, despite Apulia being the first Italian region for installed power, as can be seen from Table 5, the perception of the Apulian population on the presence of this type of plant in the area is not unequivocally clear and there is often no lack of protest movements against their construction.

Maggi et al. [54] conducted a sociological survey on the implications of the exploitation of the wind source through the construction of Wind Farms in the Sub-Apennine Dauno in Apulia. What emerged is that approximately 53.9 % of the analyzed sample did not have a clear position on the exploitation of the wind source, while 22.4 % are against the wind project, with even 5.9 % of the sample ready for active opposition in case of construction of new Wind farms.

Finally, it can be noted that since 2006, in both national and regional scenarios, the construction of solar and wind power plants has experienced strong growth, especially as regards photovoltaics. This growth was mainly caused by the strong economic incentives put in place by the Italian Government in support of the RER, which accelerated their process of technological development, laying the foundations for the level of technological maturity reached today.

The results demonstrate that for an ever-increasing use of RER to achieve the objectives related to the energy transition, it is necessary to combine the traditional technologies analyzed with alternative solutions that can reduce the impact on land consumption. Despite some barriers that still hinder its diffusion [55], offshore wind farms can contribute to reducing land consumption in exploiting wind resource.

The use of exploitation of the surfaces of buildings [51], as well as the creation of floating solar systems, for example on water surfaces of

hydropower plant [56], and the use of emerging solutions such as the creation of the photovoltaic pavement which can count on a vast availability of roadways [57], they can instead contribute to decreasing land consumption in the exploitation of solar resources.

6. Economic analysis

This section presents the economic feasibility analysis of the project. The RETScreen Expert software [12] was used to develop the economic feasibility analysis.

In particular, the feasibility analysis conducted is based on the calculation of two financial indicators the Net Present Value (NPV) and Internal Rate of Return (IRR). Starting from these two indexes, the ideal selling price of Hydrogen is obtained in order to make the project profitable.

To better evaluate the influence of scale economy on the project, two Case Studies have been analyzed: **Case A** based on a 50 MW PV Solar Plant and a 50 MW Wind Farm and **Case B** composed by a 100 MW PV Solar Plant and a 100 MW Wind Farm.

The RER Power Plant Annual Input data and Economic Input data used to develop the feasibility analysis are collected in Table 8.

For **Case A,** the data show that to repay the project, the hydrogen produced must be sold at a price not inferior to 248 €/MWh, resulting in an IRR pre-tax equal to the Discount rate. The sensitivity analyses of IRR pre-tax to the selling price of Hydrogen and to the total cost of the production plant, assuming to sell Hydrogen at 248 €/MWh, are shown in Fig. 8 **(a)** and **(c)** respectively.

On the other hand, for Case B, a payback price of 227 €/MWh results. The sensitivity analyses of IRR pre-tax to the selling price of Hydrogen and to the total cost of the production plant, assuming to sell Hydrogen at 227 €/MWh, are shown in Fig. 8 **(b)** and **(d)** respectively.

In Fig. 9, it can be observed how the different economic variables have an impact on the NPV calculation. To account for any possible combination of the input economic data on the financial indicator, a Monte Carlo analysis is performed. By studying the components of NPV calculation for Case A and Case B, it results that the percentage composition of the cost items and revenue items differs minimally with the size of the plant. This result affects the Monte Carlo analysis, since the values in Fig. 9 are the same for both Case A and Case B.

In Fig. 9 it can be inferred the results of the Monte Carlo simulation performed by the software RETScreen [12] to assess the weight of each parameter in the variability of the NPV calculation. The X axis of the graph is dimensionless and represents a relative indication of the impact of each parameter, while its sign indicates a correlation between the parameter and the NPV calculation. There is a positive correlation in fact if an increase of the parameter will increase the NPV. For the present case study, the Hydrogen exported to the grid and the Hydrogen export rate have major positive effects, meanwhile, the Initial costs have a major negative impact.

Analyzing, instead, the composition of the total costs, it is interesting to note how the initial cost is largely influenced by the specific investment cost of the Wind Farms of 2,215 €/kW for **Case A** and 2,022 €/kW for **Case B**, against 1,276 €/kW for **Case A** and 1,156 €/kW for **Case B** of PV Farms [12]. However, for the case study under examination, a higher Capacity Factor is found equal to about 28.2 % for the Wind Farm, while for the PV Farm, it is found to be 14.4 %. The Capacity Factor is defined as by (Eq. (28)).

$$\frac{E_{pp}}{P_{rated} \bullet T} \tag{28}$$

This, therefore, translates into a higher quantity of energy produced and therefore a higher production of hydrogen by the Wind Farms compared to the PV Farms. For **Case A** are obtained 19,803,043 Sm^3/y and 39,605,927 Sm^3/y for **Case B** of hydrogen deriving from the exploitation of the wind source, against 10,011,095 Sm^3/y for **Case A** and 20,022,190 Sm^3/y for **Case B** from the solar source.

There is therefore a trade-off between the investment costs of the two plant solutions and the quantity of hydrogen produced. Therefore, in order to understand which solution is more economically advantageous, a feasibility analysis is carried out, first considering only the production of hydrogen from PV farms scaled on plants of sizes from 100 MW to 200 MW, then the same analysis is performed on Wind Farms with the same nominal powers. According to the analyzed cases, the new plant scheme, therefore, envisages the expansion of the number of PV modules or wind turbines, so as to compensate for the share of energy produced by the excluded source with respect to the scheme in Fig. 4. The modules of the new plant configuration will retain the characteristics expressed in Table 2, while the new wind turbines will have the same characteristics indicated in Table 3. The economic feasibility analysis also in this case takes into account the same parameters indicated in Table 8. The results of this analysis are reported in Table 9.

What can be deduced by analyzing the values in Table 9 is that the most advantageous configuration is the 200 MW Wind farm, which despite having the highest investment and O&M costs, is the most economically advantageous as it has the lowest hydrogen selling price, equal to 222 €/MWh. The configuration proposed in **Case B** is the one immediately following as the lowest selling price, equal to a value of 227 €/MWh. The highest selling prices are recorded in the nominal power range of the plants equal to 100 MW, in particular, the highest selling price of Hydrogen is recorded in **Case A** equal to 248 €/MWh. This result highlights the existence of scale economies which therefore favor the creation of large plants to obtain reductions in plant construction and O&M costs.

To better evaluate the results in Table 9 they are compared with the hydrogen production cost values in literature. Benghanem et al. [58] analyse different hydrogen production methods from RER presenting the relative production costs. Table 10 summarizes the results of this analysis and confirms the accordance with the values obtained in Table 9.

Regarding the possibility of creating a hybrid RER solution for hydrogen production such as the wind and solar plant realized in **Case A** or **Case B**, Khouya [60] investigates a concentrated photovoltaic solar plant (CPV) combined with a wind farm that produces hydrogen feeding an alkaline water electrolyzer. The analysis is performed on five scenarios: the first scenario 1 is a 120 MW CPV plant; the second scenario is composed by a 90 MW CPV and a 30 MW Wind Farm; in the third scenario, a capacity of 60 MW CPV and a 60 MW Wind Farm is installed; the fourth scenario considers a capacity of 30 MW CPV and a 90 MW Wind Farm and in the fifth scenario a 120 MW Wind Farm is considered. The analysis results show how the configuration proposed in the fifth scenario is able to achieve the lowest hydrogen production cost followed by the configuration proposed respectively in the first and the fourth

Table 8
Technical and economic input data.

		Case A	Case B
Power Plant Annual Input data	Energy produced by PV Solar System	62,950 MWh	125,900 MWh
	Energy produced by Wind Farm	124,522 MWh	249,043 MWh
	Energy supplied to Compressors	1,712 MWh	3,134 MWh
	AWE efficiency	53 %	
	Hydrogen produced (70 bar)	28,229,206 Sm^3	56,458,256 Sm^3
Economic Input data	Total Initial Cost	216,928,304 €	398,818,696 €
	Total O&M Cost	4,920,558 €/y	8,982,539 €/y
	Inflation rate	2 %	
	Discount rate	10 %	
	Reinvestment rate	9 %	
	Debt ratio	70 %	
	Debt interest rate	7 %	
	Debt term	10 y	
	Project life	25 y	

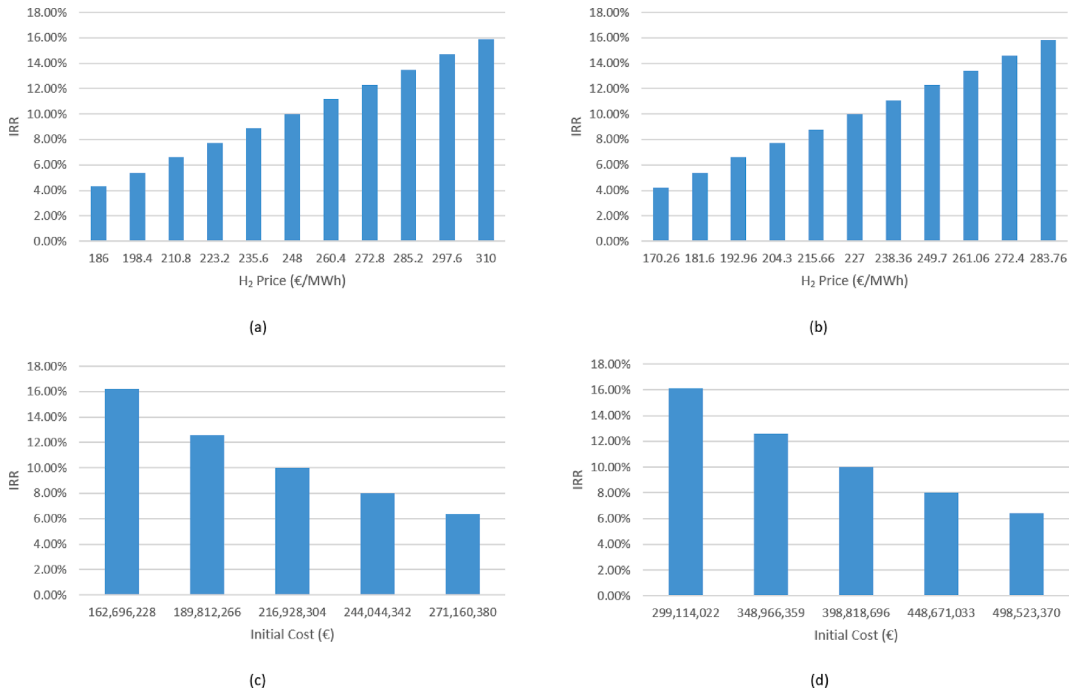

Fig. 8. Case A: (a) IRR pre-tax variation with H2 price (c) IRR pre-tax variation with Initial Cost with 248 €/MWh H2 export rate, Case B: (b) IRR pre-tax variation with H2 price (d) IRR pre-tax variation with Initial Cost with 248 €/MWh H2 export rate.

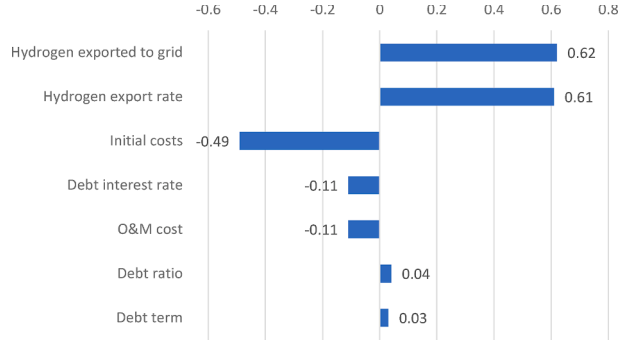

Fig. 9. Results of the economic variables impact analysis on NPV calculation.

Table 9
Comparison between the different plant solutions.

RER Power Plant	Initial Cost [€]	O&M Cost [€/y]	Hydrogen Produced [Sm^3/y]	Hydrogen Price [€/MWh]
Case A	216,928,304	4,920,558	28,229,206	248
Case B	398,818,696	8,982,539	56,458,256	227
100 MW PV farm	156,268,946	1,916,716	18,523,496	240
200 MW PV farm	303,417,943	3,557,798	37,046,833	232
100 MW Wind farm	264,738,900	7,739,826	37,934,750	241
200 MW Wind farm	487,099,501	14,231,645	75,869,520	222

scenarios in accordance with the results obtained by the present paper.

Finally, it is useful to refer to the trend in the price of Natural Gas, which represents the threshold for which Hydrogen produced from RER can obtain market shares, Fig. 10 shows the trend in the average monthly price of gas in Italy in the period from 2015 to 2022.

Table 10
Comparison between the different plant solutions[58,59].

Power Plant	Hydrogen Cost [€/MWh]
Wind	162–246
Solar	105–491
Biomass	37–214
Geothermal	33–134
Nuclear	67–168
Natural gas	42–107
Coal	26–58

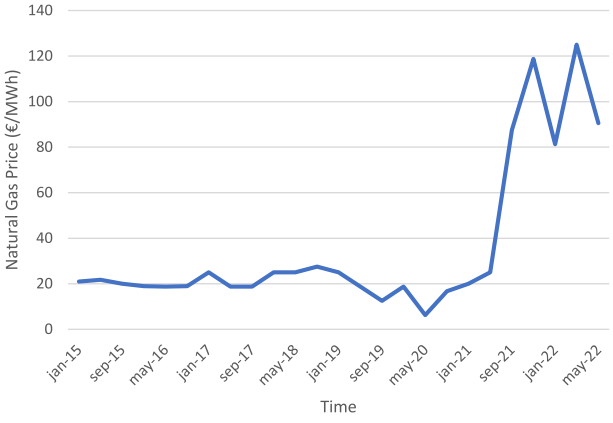

Fig. 10. Monthly Natural Gas Price in Italy [61].

From Fig. 10 it is evident that the production price of Hydrogen with the proposed method is still far from the selling prices of Natural Gas, which, in the 7 years of analysis considered, showed a maximum of around 125 €/MWh.

6.1. CO_2 reduction economic analysis

A particular consideration has been made on the environmental value of producing Hydrogen by RER. As the Global demand for hydrogen is satisfied for 83 % by fossil fuels, the development of "green" hydrogen can have a considerable impact on greenhouse gas emissions. Considering **Case A** and **Case B** the CO_2 reduction is respectively 23,371 ton/y and 54,742 t/y.

In the European Union, Directive 2003/87/EC of the European Parliament and the Council establishes the first scheme for the European greenhouse gas emission allowance. This Directive was the first step in the creation of a market for greenhouse emissions, which resulted in the European Energy Exchange (EEX) auction platform. In December 2022 the Average Auction Clearing Price was 86.76 €/t of CO_2 [62]. Considering the CO_2 emissions price as 86.76 €/ton, the results in Table 9 are modified and the new results are reported in Table 11.

The hypotheses used for the economic analysis are the same in Table 8 and for the CO_2 Average Auction Clearing Price has been estimated an annual reduction credit escalation rate of the 4 %. The hypothesis is consistent with an annual inflation rate of 2 % and with the European Green Deal which is the EU's strategy to reach the climate neutrality by 2050. Under this scenario, it results a decrease in the hydrogen price which in the 200 MW Wind farm reaches 191.2 €/MWh.

The results of the analysis conducted therefore establish a hydrogen price between 8.26 €/kg and 7.41 €/kg in the case study without incentives for CO_2 abatement and between 7.23 €/kg and 6.37 €/kg in the case in which the CO_2 Average Auction Clearing Price is considered. These results are in line with what was found by Zhou and Searle [63] who estimated in Italy an average cost of hydrogen produced from solar and wind sources equal to 8.5 €/kg, while in Europe the average cost is equal to 11 €/kg in 2020. The authors also underline how the price variation around Europe is largely caused by the renewable electricity price.

This result underlines how the influence of policies and regulation strategies can heavily influence the price formation of alternative energy carriers.

7. Conclusions

This work presents the feasibility study for the production of Hydrogen from wind and solar sources available in the Province of Brindisi, Puglia, Italy. The second and third sections analyzed the GHI and wind speed data from the site of interest. The fourth section analyzed the technologies chosen for the production of Hydrogen. In particular, as regards the solar resource, monocrystalline silicon PV technology was chosen, while for the wind resource, a wind farm consisting of horizontal axis onshore wind turbines was chosen. Finally, AWE technology was chosen for the conversion of the electricity produced by the RER.

Linked to the RER exploitation there is the technical and social issue of land consumption. An analysis of the land consumption has been carried out starting from the year 2000 to 2050. The results show how the process of urbanization is fed by the rural lands; this land class is also the one that is used for the development and construction of RER power plant. Starting from the year 2006 the RER power plant had a sharp increase thanks to the incentives and policies adopted by the Italian Government. However, the exploitation of the RER at the current rate will yield in 2050 the disappearance of about 1,2 million hectares of rural land and this number could be higher if the policies for the energy transition will speed up on the RER harnessing. The same analysis is scaled down for the Apulia Region and the results obtained show a reduction of the agricultural land up to 60,000 ha. As for the National Case, the Region Apulia data show a higher conversion of the rural land in PV farms than Wind Farms. This trend is explained by the opposition of public opinion and by the stricter regulation need for the construction of new Wind Farms. The rural land deployment could lead to a different environment, social and economic issues such as the disappearance of animal species, difficulties in the deployment and supplies of food, etc.

Finally, in the last section, an economic analysis of the project was presented. The economic feasibility is evaluated both for the 100 MW and 200 MW RER power plants. The results of the analysis estimate a minimum selling price of the hydrogen produced equal to 248 €/MWh for the 100 MW RER power plant and to 227 €/MWh for the case of 200 MW.

To better investigate the scale economies and the trade-off between the high investment-specific cost and the Capacity Factor of the Wind Farms, an additional analysis is carried out on a 200 MW and 100 MW Wind farms and PV Farms. The results show that the 200 MW Wind farm is the better economic solution for the production of hydrogen by RER obtaining a hydrogen selling price equal to 222 €/MWh. Finally, it is interesting to note that for both Wind and PV farms, the selling price is higher for the 100 MW configuration than any other examined technology 200 MW combination confirming the existence of scale economies. These prices are still far from the selling price of Natural Gas which in the last 7 years has recorded a maximum average monthly price of around 125€/MWh.

Nevertheless, whenever in the former analysis is considered the CO_2 Average Auction Clearing Price, the scenario changes significantly, showing a decrease of the hydrogen price. The two best technical solutions for the realization of hydrogen produced by RER are still the 200 MW Wind farm and the solution proposed in Case B, obtaining a hydrogen selling price respectively of 191.2 €/MWh and 197 €/MWh.

However, it is worth noting that the price of natural gas has grown sharply in recent years, partly due to geopolitical reasons. Nonetheless, the environmental issue is pushing in the direction of a substantial change in the economy and technology based on fossil fuels. All this is driving many governments to make decisions, both from a regulatory point of view and from an investment in research point of view, in order to be able to develop alternative and more Eco-sustainable technologies. Indeed, the results of the analysis reveal how the objective of an economy based on green hydrogen requires a large exploitation of RER which needs to be sustained by less consuming land technical solutions such as offshore plants, exploitation of the surfaces of buildings, waters surfaces of hydropower plants and photovoltaic pavements. Furthermore, this study has demonstrated how the widespread use of these technologies must be supported by incentive regulatory mechanisms, such as those promoted by the European Union Directive 2003/87/EC, in order to achieve the goal of an economy based on green hydrogen. Starting from these considerations, the trend of the proposed prices will undergo further changes over the next few years, thus making possible solutions that are not feasible today.

Table 11
Hydrogen Price considering the revenues for CO_2 reduction.

RER Power Plant	Gross annual CO_2 reduction [t/y]	Hydrogen Price [€/MWh]
Case A	23,371	217
Case B	54,742	197
100 MW PV farm	18,381	209
200 MW PV farm	36,763	201
100 MW Wind farm	36,360	211
200 MW Wind farm	72,721	191

CRediT authorship contribution statement

Gianpiero Colangelo: Writing – review & editing, Writing – original draft, Supervision, Methodology, Investigation, Formal analysis, Conceptualization. **Gianluigi Spirto:** Writing – review & editing, Writing – original draft, Validation, Formal analysis, Data curation. **Marco Milanese:** Writing – original draft, Validation, Formal analysis, Conceptualization. **Arturo de Risi:** Writing – original draft, Supervision, Methodology, Funding acquisition, Conceptualization.

Declaration of competing interest

The authors declare that they have no known competing financial interests or personal relationships that could have appeared to influence the work reported in this paper.

Data availability

Data will be made available on request.

References

[1] IEA (2022). Hydrogen – analysis; 2022. https://www.iea.org/reports/hydrogen.
[2] IEA (2021), Global Hydrogen Review 2021; 2021. https://www.iea.org/reports/global-hydrogen-review-2021.
[3] Borgstedt P, Neyer B, Schewe G. Paving the road to electric vehicles – a patent analysis of the automotive supply industry. J Clean Prod 2017;167:75–87. https://doi.org/10.1016/j.jclepro.2017.08.161.
[4] Asif U, Schmidt K. Fuel Cell Electric Vehicles (FCEV): policy advances to enhance commercial success. Sustainability 2021;13:5149. https://doi.org/10.3390/su13095149.
[5] Chiesa P, Lozza G, Mazzocchi L. Using hydrogen as gas turbine fuel. J Eng Gas Turbines Power 2005;127:8. https://doi.org/10.1115/1.1787513.
[6] Xiao H, Valera-Medina A, Bowen PJ. Modeling combustion of ammonia/hydrogen fuel blends under gas turbine conditions. Energy Fuels 2017;31:8631–42. https://doi.org/10.1021/acs.energyfuels.7b00709.
[7] Incer-Valverde J, Patiño-Arévalo LJ, Tsatsaronis G, Morosuk T. Hydrogen-driven Power-to-X: State of the art and multicriteria evaluation of a study case. Energ Conver Manage 2022;266:115814. https://doi.org/10.1016/j.enconman.2022.115814.
[8] Hafsi O, Abdelkhalek O, Mekhilef S, Soumeur MA, Hartani MA, Chakar A. Integration of hydrogen technology and energy management comparison for DC-Microgrid including renewable energies and energy storage system. Sustain Energy Technol Assess 52 Part B 2022. https://doi.org/10.1016/j.seta.2022.102121.
[9] Oldenbroek V, Smink G, Salet T, van Wijk AJM. Fuel cell electric vehicle as a power plant: techno-economic scenario analysis of a renewable integrated transportation and energy system for smart cities in two climates. Appl Sci 2019;10:143. https://doi.org/10.3390/app10010143.
[10] Temiz M, Dincer I. Development of solar and wind based hydrogen energy systems for sustainable communities. Energ Conver Manage 2022;269:116090. https://doi.org/10.1016/j.enconman.2022.116090.
[11] GSE, Consumi finali lordi di energia da fonti rinnovabili e totali nella Regione Puglia, 2022. https://www.gse.it/dati-e-scenari/monitoraggio-fer/monitoraggio-regionale/Puglia.
[12] RETScreen Expert; n.d.
[13] The low emissions analysis platform; n.d.
[14] ENEA, Global Horizontal Irradiance, daily monthly averaged and annual values, 243 location, (n.d.). http://www.solaritaly.enea.it/TabelleRad/TabelleRadEn.php.
[15] Hay JE. Calculation of monthly mean solar radiation for horizontal and inclined surfaces. Sol Energy 1979;23:301–7. https://doi.org/10.1016/0038-092X(79)90123-3.
[16] Ahmad GE, Hussein HMS, El-Ghetany HH. Theoretical analysis and experimental verification of PV modules. Renew Energy 2003;28:1159–68. https://doi.org/10.1016/S0960-1481(02)00228-8.
[17] Bataineh K, Dalalah D. Optimal configuration for design of stand-alone PV System. SGRE 2012;03:139–47. https://doi.org/10.4236/sgre.2012.32020.
[18] Milanese M, Tornese L, Colangelo G, Laforgia D, de Risi A. Numerical method for wind energy analysis applied to Apulia Region, Italy. Energy 2017;128:1–10. https://doi.org/10.1016/j.energy.2017.03.170.
[19] Scire J, Robe F, Fernaua M, Yamartno R. A user's guide for the CALMET meteorological model; 2000.
[20] International Electrotechnical Commission (IEC). IEC 61400–1 Wind energy generation systems – Part 1: Design requirements. Edition 2019;4.
[21] Kassem Y, Çamur H, Aateg RAF. Exploring solar and wind energy as a power generation source for solving the electricity crisis in Libya. Energies 2020;13:3708. https://doi.org/10.3390/en13143708.
[22] Kassem Y, Gökçekuş H, Zeitoun M. Modeling of techno-economic assessment on wind energy potential at three selected coastal regions in Lebanon. Model Earth Syst Environ 2019;5:1037–49. https://doi.org/10.1007/s40808-019-00589-9.
[23] Khan MA, Çamur H, Kassem Y. Modeling predictive assessment of wind energy potential as a power generation sources at some selected locations in Pakistan. Model Earth Syst Environ 2019;5:555–69. https://doi.org/10.1007/s40808-018-0546-6.
[24] Kassem Y, Camur H, Abughinda SAM, Sefik A. Wind energy potential assessment in selected regions in Northern Cyprus Based on Weibull Distribution Function. J Eng Appl Sci 2019;15:128–40. https://doi.org/10.36478/jeasci.2020.128.140.
[25] Okorie ME, Inambao F, Chiguvare Z. Evaluation of wind shear coefficients surface roughness and energy yields over Inland Locations in Namibia. Proc Manuf 2017;7:630–8. https://doi.org/10.1016/j.promfg.2016.12.094.
[26] Gualtieri G, Secci S. Methods to extrapolate wind resource to the turbine hub height based on power law: A 1-h wind speed vs. Weibull distribution extrapolation comparison. Renew Energy 2012;43:183–200. https://doi.org/10.1016/j.renene.2011.12.022.
[27] Haeseldonckx D, Dhaeseleer W. The use of the natural-gas pipeline infrastructure for hydrogen transport in a changing market structure. Int J Hydrogen Energy 2007;32:1381–6. https://doi.org/10.1016/j.ijhydene.2006.10.018.
[28] Wang H, Tong Z, Zhou G, Zhang C, Zhou H, Wang Y, et al. Research and demonstration on hydrogen compatibility of pipelines: a review of current status and challenges. Int J Hydrogen Energy 2022;47:28585–604. https://doi.org/10.1016/j.ijhydene.2022.06.158.
[29] American Society of Mechanical Engineers, Asme B31G. 12-2019 hydrogen piping and pipelines ASME code for pressure piping; 2019.
[30] Snam, Snam: hydrogen blend doubled to 10% in Contursi trial, Snam.It (2020). https://www.snam.it/en/media/news-and-press-releases/news/2020/snam-hydrogen-blend-doubled-to-10–in-contursi-trial.html (accessed January 18, 2024).
[31] Cerniauskas S, Jose Chavez Junco A, Grube T, Robinius M, Stolten D. Options of natural gas pipeline reassignment for hydrogen: Cost assessment for a Germany case study. Int J Hydrogen Energy 2020;45: 12095–107. https://doi.org/10.1016/j.ijhydene.2020.02.121.
[32] Jiang L, Cui S, Sun P, Wang Y, Yang C. Comparison of monocrystalline and polycrystalline solar modules. In: 2020 IEEE 5th Information Technology and Mechatronics Engineering Conference (ITOEC), IEEE, Chongqing, China; 2020. p. 341–344. https://doi.org/10.1109/ITOEC49072.2020.9141722.
[33] Zhang S, He Y. Analysis on the development and policy of solar PV power in China. Renew Sustain Energy Rev 2013;21:393–401. https://doi.org/10.1016/j.rser.2013.01.002.
[34] Gestore dei Servizi Energetici, Il Punto sull'eolico; 2017. https://www.gse.it/documenti_site/Documenti%20GSE/Studi%20e%20scenari/Il%20punto%20sull%27eolico.pdf.
[35] Imran A, Imanova GT, Mbianda XY, Alharbi OML. Role of the radiations in water splitting for hydrogen generation. Sustain Energy Technol Assess 2022;51. https://doi.org/10.1016/j.seta.2021.101926.
[36] Chi J, Yu H. Water electrolysis based on renewable energy for hydrogen production. Chin J Catal 2018;39:390–4. https://doi.org/10.1016/S1872-2067(17)62949-8.
[37] Burton NA, Padilla RV, Rose A, Habibullah H. Increasing the efficiency of hydrogen production from solar powered water electrolysis. Renew Sustain Energy Rev 2021;135:110255. https://doi.org/10.1016/j.rser.2020.110255.
[38] Wolf SE, Winterhalder FE, Vibhu V, (Bert) De Haart LGJ, Guillon O, Eichel RA, Menzler NH. Solid oxide electrolysis cells – current material development and industrial application. J Mater Chem 2023;A 11: 17977–18028. https://doi.org/10.1039/D3TA02161K.
[39] Ulleberg O. Modeling of advanced alkaline electrolyzers: a system simulation approach. Int J Hydrogen Energy 2003;28:21–33. https://doi.org/10.1016/S0360-3199(02)00033-2.
[40] Hernández-Gómez Á, Ramirez V, Guilbert D. Investigation of PEM electrolyzer modeling: Electrical domain, efficiency, and specific energy consumption. Int J Hydrogen Energy 2020;45:14625–39. https://doi.org/10.1016/j.ijhydene.2020.03.195.
[41] El-Shafie M. Hydrogen production by water electrolysis technologies: A review. Results Eng 2023;20:101426. https://doi.org/10.1016/j.rineng.2023.101426.
[42] Mohammadi A, Mehrpooya M. A comprehensive review on coupling different types of electrolyzer to renewable energy sources. Energy 2018;158:632–55. https://doi.org/10.1016/j.energy.2018.06.073.
[43] Ramaswamy N, Mukerjee S. Alkaline anion-exchange membrane fuel cells: challenges in electrocatalysis and interfacial charge transfer. Chem Rev 2019;119:11945–79. https://doi.org/10.1021/acs.chemrev.9b00157.
[44] F.M. Sapountzi, J.M. Gracia, C.J. (Kees-J. Weststrate, H.O.A. Fredriksson, J.W. (Hans) Niemantsverdriet, Electrocatalysts for the generation of hydrogen, oxygen and synthesis gas, Progress in Energy and Combustion Science 58 (2017) 1–35. https://doi.org/10.1016/j.pecs.2016.09.001.
[45] A. Agrillo, V. Surace, P. Liberatore, Rapporto Statistico - Solare Fotovoltaico 2021, (2022). https://www.gse.it/documenti_site/Documenti%20GSE/Rapporti%20statistici/Solare%20Fotovoltaico%20-%20Rapporto%20Statistico%202021.pdf.
[46] Milanese M, Congedo PM, Colangelo G, Lala R, Laforgia D, de Risi A. Numerical method for wind energy analysis in WTG siting. Renew Energy 2019;136:202–10. https://doi.org/10.1016/j.renene.2018.12.125.
[47] Ohl C, Eichhorn M. The mismatch between regional spatial planning for wind power development in Germany and national eligibility criteria for feed-in tariffs—A case study in West Saxony. Land Use Policy 2010;27:243–54. https://doi.org/10.1016/j.landusepol.2009.06.004.
[48] Geneletti D. Biodiversity Impact Assessment of roads: an approach based on ecosystem rarity. Environ Impact Assess Rev 2003;23:343–65. https://doi.org/10.1016/S0195-9255(02)00099-9.
[49] Kabisch N, Frantzeskaki N, Pauleit S, Naumann S, Davis M, Artmann M, et al. Nature-based solutions to climate change mitigation and adaptation in urban areas: perspectives on indicators, knowledge gaps, barriers, and opportunities for action. E&S 2016;21:art39. https://doi.org/10.5751/ES-08373-210239.
[50] Ronchi E, Leoni S, Vigni F, Pettinao E, Galli L, Erme A, et al. 4th Report on Circular Economy in Italy; 2022. https://circulareconomynetwork.it/rapporto-2022/.
[51] M. Munafò, Consumo di suolo, dinami-che territoriali e servizi ecosistemici, (2022).
[52] ISPRA, Territorio - Processi e Trasformazioni in Italia, in: 2018th ed.; 2018.
[53] IEA, Renewables Information; 2022.
[54] M. Maggi, Gli impianti eolici nella percezione di alcune comunità del Sub-Appenino Dauno., (2015).

[55] Wu Y, Liu F, Wu J, He J, Xu M, Zhou J. Barrier identification and analysis framework to the development of offshore wind-to-hydrogen projects. Energy 2022;239:122077. https://doi.org/10.1016/j.energy.2021.122077.
[56] Ateş AM. Unlocking the floating photovoltaic potential of Türkiye's hydroelectric power plants. Renew Energy 2022;199:1495–509. https://doi.org/10.1016/j.renene.2022.09.096.
[57] Li S, Ma T, Wang D. Photovoltaic pavement and solar road: A review and perspectives. Sustainable Energy Technol Assess 2023;55:102933. https://doi.org/10.1016/j.seta.2022.102933.
[58] Benghanem M, Mellit A, Almohamadi H, Haddad S, Chettibi N, Alanazi AM, et al. Hydrogen production methods based on solar and wind energy: a review. Energies 2023;16:757. https://doi.org/10.3390/en16020757.
[59] El-Emam RS, Özcan H. Comprehensive review on the techno-economics of sustainable large-scale clean hydrogen production. J Clean Prod 2019;220:593–609. https://doi.org/10.1016/j.jclepro.2019.01.309.
[60] Khouya A. Levelized costs of energy and hydrogen of wind farms and concentrated photovoltaic thermal systems. A case study in Morocco. Int J Hydrogen Energy 2020;45:31632–50. https://doi.org/10.1016/j.ijhydene.2020.08.240.
[61] Gracceva F, Baldissara B, Colosimo A, Zini A. Analisi Trimestrale del Sistema Energetico Italiano - I Trimestre 2022. ENEA 2022:34.
[62] European Energy Exchange, Auctions by the Common Auction Platform - October, November, December 2022, (2023). https://climate.ec.europa.eu/system/files/2023-03/cap_report_202212_en.pdf.
[63] Zhou Y, Searle S. Cost of renewable hydrogen produced onsite at hydrogen refueling stations in Europe, International Council on Clean Transportation; n.d.